

Published in final edited form as:

Science. 2015 July 17; 349(6245): 316–320. doi:10.1126/science.aaa8064.

Neutrophil extracellular traps license macrophages and Th17 cells for cytokine production in atherosclerosis

Annika Warnatsch, Marianna Ioannou, Qian Wang, and Venizelos Papayannopoulos

The Francis Crick Institute Mill Hill Laboratory, The Ridgeway, London, NW7 1AA, UK

Abstract

Secretion of the cytokine interleukin-1 β (IL-1 β) by macrophages, a major driver of pathogenesis in atherosclerosis, requires two steps. First, priming signals promote transcription of immature IL-1 β and then, endogenous “danger” signals activate innate immune signaling complexes called inflammasomes, to process IL-1 β processing for secretion. While cholesterol crystals act as danger signals in atherosclerosis, what primes IL-1 β transcription remains elusive. Using a murine model of atherosclerosis, we show that cholesterol crystals acted both as priming and danger signals for IL-1 β production. Cholesterol crystals triggered neutrophils to release neutrophil extracellular traps (NETs). NETs primed macrophages for cytokine release, activating Th-17 cells that amplify immune cell recruitment in atherosclerotic plaques. Therefore, danger signals may drive sterile inflammation, such as that seen in atherosclerosis, through their interactions with neutrophils.

Inflammation is critical against infection but must be regulated by multiple checkpoints to prevent inflammatory disease (1). During infection, cytokine transcription is triggered by microbial molecules that activate pattern recognition receptors (2). Release of mature active cytokines requires additional “danger” signals associated with host cell damage. Known as danger-associated molecular patterns (DAMPs), these secondary signals activate the NLRP3 and other inflammasomes, promoting cleavage and activation of the protease caspase-1 that processes cytokines such as interleukin-1 β (IL-1 β) into their mature form (3).

IL-1 β plays a critical role in the development of atherosclerosis and other inflammatory diseases. Due to its low solubility, cholesterol crystalizes in circulation and is taken up by monocyte-derived macrophages (4–6) activating their inflammasomes to release IL-1 β and other proinflammatory cytokines (7). These molecules recruit myeloid cells to vascular endothelium where their cholesterol content generates obstructive lesions (8). In atherosclerosis and other sterile inflammatory diseases, the endogenous priming signals that activate IL-1 β transcription prior to inflammasome activation remain unknown.

IL-1 β upregulates chemokines that recruit neutrophils to atherosclerotic lesions (9–11). Neutrophils are implicated in disease (12, 13) but their role in pathogenesis remains poorly understood. To combat pathogens that evade phagocytosis (14), neutrophils release neutrophil extracellular traps (NETs) composed of decondensed chromatin and

antimicrobials (15). While NETs are implicated in several inflammatory diseases (16), their pathogenic mechanism and role in atherosclerosis are unclear.

To examine how neutrophils respond during atherosclerosis we investigated the effect of cholesterol crystals on human blood-derived neutrophils. Cholesterol crystals induced NETosis (Fig. 1A and B) at concentrations required to activate the inflammasome (Fig. S1A and B) (7) as efficiently as microbes (14), triggering a reactive oxygen species (ROS) burst (Fig. S1C) and neutrophil elastase (NE) translocation to the nucleus (Fig. S1D), a critical step for NETosis (17). NETosis depended on ROS as it was blocked by the NADPH oxidase inhibitor diphenylene iodonium (DPI) or an inhibitor (NEi) of the neutrophil-specific proteases NE and proteinase 3 (PR3) (17) but not by Cl-amidine which inhibits peptidylarginine deiminase (PAD) enzymes implicated in NETosis (18) (Fig. 1A, B and S1E). Consistently, DPI or NEi blocked NE translocation to the nucleus driven by cholesterol (Fig. S1D) (19).

Next, we examined whether NETs form during atherosclerosis. Previous studies reported the presence of NETs in lesions but showed intact neutrophils with condensed nuclei (20) or luminal rather than lesion-associated neutrophils in the absence of specific NET markers (21). We detected NETs as large amorphous extracellular structures in atherosclerotic lesions from apolipoprotein E (ApoE) mice that were placed on high fat diet (HFD) for 8 weeks to induce hypercholesterolemia (Fig. 1C). NETs formed in cholesterol-rich areas but were absent from adjacent adventitia (Fig. S2A). To block NETosis *in vivo*, we crossed ApoE deficient animals with mice deficient in NE and PR3 since deleting both enzymes may abrogate NETosis more effectively (22). NETs were completely absent in lesions of ApoE/NE/PR3 deficient mice after 8 weeks on HFD (Fig. 1C) and ApoE-deficient mice after 6 weeks on HFD receiving DNase, which degrades NETs (23) (Fig. S2B).

Next, we assessed the effect of NET deficiency on atherosclerosis. When placed on HFD, ApoE and ApoE/NE/PR3 deficient mice exhibited similar weight gain (Fig. S3A) and blood cholesterol, triglyceride and LDL concentrations (Fig. S3B). Analysis of aortic root cross-sections showed that the two groups were modestly different after 4 weeks on HFD (Fig. S3C and D) suggesting that NETs did not play a critical role early during atherogenesis. However, after 8 weeks on HFD, ApoE/NE/PR3 deficient mice exhibited a 3-fold reduction in plaque size relative to ApoE deficient controls (Fig. 2A and B). These differences were also reflected by *en face* analysis of intact aortas (Fig. S3E and F). DNase injections to ApoE deficient mice on HFD for 6 weeks resulted in a comparable 3-fold reduction in lesion size, excluding that the proteases played NET-independent roles (Fig. 2B and C). Lesion growth was unaffected by DNase in ApoE/NE/PR3 deficient mice that lack NETs.

NET-deficient mice exhibited a reduction in lesion growth that was comparable to mice lacking NLRP3 or the IL-1 receptor, suggesting that NETs may drive atherosclerosis by modulating cytokine production. Indeed, IL-1 α , IL-1 β and IL-6 were elevated in the plasma of ApoE deficient animals after 8 weeks on HFD, but were largely absent in ApoE/NE/PR3 deficient mice (Fig. 3A and S4A). After 16 weeks on HFD, IL-1 α but not IL-1 β concentrations were still elevated in ApoE deficient controls compared to NET deficient animals (Fig. S4B). DNase administration abrogated plasma cytokine concentrations in

ApoE deficient controls but had no effect on ApoE/PR3/NE mice (Fig. S4C). Furthermore, IL-1 β staining, which detects both immature and mature protein, was prominent in lesions from ApoE deficient mice but absent in ApoE/NE/PR3 knockout animals and colocalized with NETs and macrophages (Fig. 3B and Fig. S4D). By contrast, IL-1 β concentrations were similar in the spleen or in blood mononuclear cells (Fig. S4E), although we cannot exclude that systemic cytokines were not produced differentially elsewhere. In addition, IL-1 β mRNA concentrations were significantly reduced in aortas from ApoE/PR3/NE deficient mice (Fig. 3C). Together, these data exclude that NE and PR3 were mediating IL-1 β maturation post-translationally and instead suggest that NETs are essential for the transcription of pro-inflammatory cytokines.

The requirement of NETs for cytokine production, and proximity of NETs to macrophages (Fig. 3D) and IL-1 β in lesions (Fig. 3B) prompted us to examine whether NETs regulate cytokine production by macrophages. We prepared NETs from cholesterol crystal-stimulated neutrophils (Fig. S5A)(24) and investigated their effects on CD14-purified, blood-derived human monocytes *in vitro*. Stimulation with NETs or cholesterol crystals separately, yielded minor increases in IL-1 β and IL-6 concentrations in culture supernatants (Fig. 3E and Fig. S5B). In contrast, monocytes released substantial cytokine concentrations when pre-treated with NETs and subsequently stimulated with cholesterol crystals (Fig. 3E). By comparison, neutrophils were not a major source of cytokines as they released negligible concentrations in response to cholesterol crystals (Fig. S5C). Degradation of NETs by DNase treatment (Fig. S4A) abrogated cytokine release (Fig. S5B) indicating the requirement for a DNA moiety. Consistently, an oligonucleotide (ODN) antagonist of the pattern recognition DNA receptor Toll like receptor 9 (TLR9), significantly reduced cytokine release in NET-treated monocytes but not monocytes primed with bacterial lipopolysaccharide (LPS) (Fig. 3E). Since TLR9 is not expressed in monocytes, these data suggest that DNA is important for monocyte activation but its detection is mediated via other DNA receptors blocked by ODN. Since blocking with oligonucleotide did not fully inhibit IL-1 β induction, we reasoned that additional non-DNA NET factors contribute to monocyte activation. Blocking TLR2 and TLR4, which bind endogenous proteins, decreased IL-1 β release and synergized with oligonucleotide inhibition, indicating that both protein and DNA moieties are important in NET-mediated priming (Fig. S5D). Importantly, the complete abrogation by DNase suggests that the association of these moieties is critical. In the absence of cholesterol, NETs did not induce substantial inflammasome activation as reflected by the lack caspase-1 and IL-1 β maturation (Fig. 3F), observed only upon co-stimulation with cholesterol crystals. Stimulation with NETs also upregulated monocytic cytokine transcripts (Fig. 3G). These data are consistent with NETs providing priming signals in atherosclerosis.

IL-1 β upregulates the T cell-derived cytokine IL-17, which drives the chemokines CXCL1 and CXCL2 to promote neutrophil recruitment during inflammation (9, 25). Both groups of mice exhibited comparable T cells numbers (Fig. S6 and Fig. S7) but aortas from ApoE/PR3/NE deficient mice on 8 week HFD contained few IL-17+ T cells compared to ApoE deficient controls (Fig. 4A and B). IL-17 producing T cells could not be detected in aortas of ApoE -/- animals after 4 weeks on HFD (Fig. S8A and B), suggesting that strong T cell activation does not precede NET-driven inflammation. The blood of NET-deficient mice did not exhibit alterations in immune cell populations and circulating IL-17+ T cells were

absent in both groups (Fig. S9 and Fig. S10). The spleen and lymph nodes contained a small IL-17+ $\gamma\delta$ -T cell population but no IL-17+ $\alpha\beta$ -T cells (Fig. S11 and S12A and B). Furthermore, concentrations of IL-17A, CXCL1, CXCL2 and the monocyte chemokine CCL2 were also significantly reduced in aortas of ApoE/NE/PR3 deficient mice (Fig. 4C). Consistently, we counted fewer neutrophils in lesions and the adventitia of ApoE/NE/PR3 deficient mice, by microscopy (Fig. 4D) and FACS (Fig. S7B). While both groups contained a comparable makeup of immune cells (Fig. S7A), ApoE/NE/PR3 deficient animals had significantly lower total immune cell counts per aorta (Fig. S7B), consistent with reduced inflammation and smaller lesions. Adhesion molecule transcripts were similar in aortas from both groups but differences may be difficult to detect due to the patchy lesion morphology (Fig. S12C). Importantly, neutrophil recruitment was comparable in the skin of WT and NE/PR3 deficient animals treated with Aldara imiquimod (Fig. S13A and B) which drives IL-1 exogenously to promote sterile psoriatic inflammation (26). Hence, reduced neutrophil recruitment in ApoE/NE/PR3 deficient lesions was not due to intrinsic defects in neutrophil chemotaxis or extravasation. Therefore, NET-mediated priming of macrophages promotes a self-amplifying IL-1/IL-17 cascade and uncovers a mechanism for neutrophils to regulate Th17 cells that sustains chronic sterile inflammation (Fig. S13C).

Our data uncover a requirement of NETs as priming cues *in vivo* and show that NETs are substantially more potent in priming cytokines than activating the inflammasome. While other endogenous molecules such as oxidized LDL prime *in vitro*, their importance *in vivo* has not been demonstrated (7, 27). Interestingly, antibodies against oxidized LDL in lesions recognize oxidized phospholipids that suppress inflammation (28). Importantly, NETosis may prime more efficiently than necrosis (29, 30) as it effectively exposes highly decondensed and pro-inflammatory DNA (31).

A recent study employing Cl-amidine proposed that NETs drive a pDC-derived interferon- α (IFN- α) autoimmune cascade in atherosclerosis via TLR9 ligation (20). However, TLR9 deficiency has little effect on atherogenesis (32). Moreover, PAD enzymes are expressed in many cell types (33) and were dispensable for NETosis triggered by cholesterol crystals (Fig. S1G). While IFN signaling downregulates IL-1 β expression, genetic ablation of the IFN α/β receptor yields a modest 25% decrease in lesion size (34) as IFNs may contribute to pathogenesis via the upregulation of caspases (3, 35, 36).

NET priming may drive inflammation in other NET-associated diseases such as cystic fibrosis and rheumatoid arthritis (24, 37). In contrast to the broad significance of IL-1 and IL-17, NETs play more specialized roles in immune defense (14) and NET-deficient individuals are only susceptible to mild fungal infection (38). Hence, blocking NETosis or degrading NETs may help treat inflammatory diseases.

SUPPLEMENTARY MATERIALS

Refer to Web version on PubMed Central for supplementary material.

ACKNOWLEDGMENTS

We thank Q. Xu for providing the *ApoE*^{-/-} mice and Z. Zhang for training, L. Mrowietz for help with NET preparations, B. Stockinger, A. Zychlinsky, A. Schaefer and M. Wilson for comments on the manuscript. This work was supported by the UK Medical Research Council MC_UP_1202/13 principally conducted at the MRC National Institute for Medical Research and completed at the Francis Crick Institute which receives its core funding from the UK Medical Research Council, Cancer Research UK and the Wellcome Trust. The data are contained in the manuscript and the supplementary materials.

References

- Lamkanfi M, Dixit VM. Mechanisms and functions of inflammasomes. *Cell*. 2014; 157:1013–1022. published online EpubMay 22. DOI: 10.1016/j.cell.2014.04.007 [PubMed: 24855941]
- Schroder K, Tschopp J. The inflammasomes. *Cell*. 2010; 140:821–832. published online EpubMar 19. DOI: 10.1016/j.cell.2010.01.040 [PubMed: 20303873]
- Latz E, Xiao TS, Stutz A. Activation and regulation of the inflammasomes. *Nature reviews. Immunology*. 2013; 13:397–411. published online EpubJun. DOI: 10.1038/nri3452
- Lessner SM, Prado HL, Waller EK, Galis ZS. Atherosclerotic lesions grow through recruitment and proliferation of circulating monocytes in a murine model. *Am J Pathol*. 2002; 160:2145–2155. published online EpubJun. DOI: 10.1016/S0002-9440(10)61163-7 [PubMed: 12057918]
- Swirski FK, Pittet MJ, Kircher MF, Aikawa E, Jaffer FA, Libby P, Weissleder R. Monocyte accumulation in mouse atherogenesis is progressive and proportional to extent of disease. *Proc Natl Acad Sci U S A*. 2006; 103:10340–10345. published online EpubJul 5. DOI: 10.1073/pnas.0604260103 [PubMed: 16801531]
- Landsman L, Bar-On L, Zernecke A, Kim KW, Krauthgamer R, Shagdarsuren E, Lira SA, Weissman IL, Weber C, Jung S. CX3CR1 is required for monocyte homeostasis and atherogenesis by promoting cell survival. *Blood*. 2009; 113:963–972. published online EpubJan 22. DOI: 10.1182/blood-2008-07-170787 [PubMed: 18971423]
- Duewell P, Kono H, Rayner KJ, Sirois CM, Vladimer G, Bauernfeind FG, Abela GS, Franchi L, Nunez G, Schnurr M, Espevik T, et al. NLRP3 inflammasomes are required for atherogenesis and activated by cholesterol crystals. *Nature*. 2010; 464:1357–1361. published online EpubApr 29. DOI: 10.1038/nature08938 [PubMed: 20428172]
- Grebe A, Latz E. Cholesterol crystals and inflammation. *Current rheumatology reports*. 2013; 15:313. published online EpubMar. doi: 10.1007/s11926-012-0313-z [PubMed: 23412688]
- Miller LS, O'Connell RM, Gutierrez MA, Pietras EM, Shahangian A, Gross CE, Thirumala A, Cheung AL, Cheng G, Modlin RL. MyD88 mediates neutrophil recruitment initiated by IL-1R but not TLR2 activation in immunity against *Staphylococcus aureus*. *Immunity*. 2006; 24:79–91. published online EpubJan. DOI: 10.1016/j.immuni.2005.11.011 [PubMed: 16413925]
- Naruko T, Ueda M, Haze K, van der Wal AC, van der Loos CM, Itoh A, Komatsu R, Ikura Y, Ogami M, Shimada Y, Ehara S, et al. Neutrophil infiltration of culprit lesions in acute coronary syndromes. *Circulation*. 2002; 106:2894–2900. published online EpubDec 3 (. [PubMed: 12460868]
- Rotzius P, Thams S, Soehnlein O, Kenne E, Tseng CN, Bjorkstrom NK, Malmberg KJ, Lindbom L, Eriksson EE. Distinct infiltration of neutrophils in lesion shoulders in *ApoE*^{-/-} mice. *Am J Pathol*. 2010; 177:493–500. published online EpubJul. DOI: 10.2353/ajpath.2010.090480 [PubMed: 20472897]
- Drechsler M, Megens RT, van Zandvoort M, Weber C, Soehnlein O. Hyperlipidemia-triggered neutrophilia promotes early atherosclerosis. *Circulation*. 2010; 122:1837–1845. published online EpubNov 2. DOI: 10.1161/CIRCULATIONAHA.110.961714 [PubMed: 20956207]
- Doring Y, Drechsler M, Wantha S, Kemmerich K, Lievens D, Vijayan S, Gallo RL, Weber C, Soehnlein O. Lack of neutrophil-derived CRAMP reduces atherosclerosis in mice. *Circulation research*. 2012; 110:1052–1056. published online EpubApr 13. DOI: 10.1161/CIRCRESAHA.112.265868 [PubMed: 22394519]
- Branzk N, Lubojemska A, Hardison SE, Wang Q, Gutierrez MG, Brown GD, Papayannopoulos V. Neutrophils sense microbe size and selectively release neutrophil extracellular traps in response to

- large pathogens. *Nat Immunol.* 2014; 15:1017–1025. published online EpubNov. DOI: 10.1038/ni.2987 [PubMed: 25217981]
15. Brinkmann V, Reichard U, Goosmann C, Fauler B, Uhlemann Y, Weiss DS, Weinrauch Y, Zychlinsky A. Neutrophil extracellular traps kill bacteria. *Science.* 2004; 303:1532–1535. published online EpubMar 5 (. [PubMed: 15001782]
 16. Branzk N, Papayannopoulos V. Molecular mechanisms regulating NETosis in infection and disease. *Seminars in immunopathology.* 2013; 35:513–530. published online EpubJul. DOI: 10.1007/s00281-013-0384-6 [PubMed: 23732507]
 17. Papayannopoulos V, Metzler KD, Hakkim A, Zychlinsky A. Neutrophil elastase and myeloperoxidase regulate the formation of neutrophil extracellular traps. *Journal of Cell Biology.* 2010; 191:677–691. DOI: 10.1083/jcb.201006052 [PubMed: 20974816]
 18. Wang YM, Li M, Stadler S, Correll S, Li PX, Wang DC, Hayama R, Leonelli L, Han H, Grigoryev SA, Allis CD, et al. Histone hypercitrullination mediates chromatin decondensation and neutrophil extracellular trap formation. *Journal of Cell Biology.* 2009; 184:205–213. DOI: 10.1083/jcb.200806072 [PubMed: 19153223]
 19. Metzler KD, Goosmann C, Lubojemska A, Zychlinsky A, Papayannopoulos V. A myeloperoxidase-containing complex regulates neutrophil elastase release and actin dynamics during NETosis. *Cell reports.* 2014; 8:883–896. published online EpubAug 7. DOI: 10.1016/j.celrep.2014.06.044 [PubMed: 25066128]
 20. Knight JS, Luo W, O'Dell AA, Yalavarthi S, Zhao W, Subramanian V, Guo C, Grenn RC, Thompson PR, Eitzman DT, Kaplan MJ. Peptidylarginine deiminase inhibition reduces vascular damage and modulates innate immune responses in murine models of atherosclerosis. *Circulation research.* 2014; 114:947–956. published online EpubMar 14. DOI: 10.1161/CIRCRESAHA.114.303312 [PubMed: 24425713]
 21. Megens RT, Vijayan S, Lievens D, Doring Y, van Zandvoort MA, Grommes J, Weber C, Soehnlein O. Presence of luminal neutrophil extracellular traps in atherosclerosis. *Thrombosis and haemostasis.* 2012; 107:597–598. published online EpubMar. DOI: 10.1160/TH11-09-0650 [PubMed: 22318427]
 22. Kessenbrock K, Froehlich L, Sixt M, Laemmermann T, Pfister H, Bateman A, Belaouaj A, Ring J, Ollert M, Faessler R, Jenne DE. Proteinase 3 and neutrophil elastase enhance inflammation in mice by inactivating antiinflammatory progranulin. *Journal of Clinical Investigation.* 2008; 118:2438–2447. published online EpubJul. DOI: 10.1172/jci34694 [PubMed: 18568075]
 23. Hakkim A, Fuernrohr BG, Amann K, Laube B, Abu Abed U, Brinkmann V, Herrmann M, Voll RE, Zychlinsky A. Impairment of neutrophil extracellular trap degradation is associated with lupus nephritis. *Proceedings of the National Academy of Sciences of the United States of America.* 2010; 107:9813–9818. published online EpubMay 25. DOI: 10.1073/pnas.0909927107 [PubMed: 20439745]
 24. Papayannopoulos V, Staab D, Zychlinsky A. Neutrophil Elastase Enhances Sputum Solubilization in Cystic Fibrosis Patients Receiving DNase Therapy. *Plos One.* 2011; 6:e28526. published online EpubDec 9. doi: 10.1371/journal.pone.0028526 [PubMed: 22174830]
 25. Park H, Li Z, Yang XO, Chang SH, Nurieva R, Wang YH, Wang Y, Hood L, Zhu Z, Tian Q, Dong C. A distinct lineage of CD4 T cells regulates tissue inflammation by producing interleukin 17. *Nat Immunol.* 2005; 6:1133–1141. published online EpubNov. DOI: 10.1038/ni1261 [PubMed: 16200068]
 26. Walter A, Schafer M, Cecconi V, Matter C, Urošević-Maiwald M, Belloni B, Schonewolf N, Dummer R, Bloch W, Werner S, Beer HD, et al. Aldara activates TLR7-independent immune defence. *Nature communications.* 2013; 4:1560.doi: 10.1038/ncomms2566
 27. Sheedy FJ, Grebe A, Rayner KJ, Kalantari P, Ramkhalawon B, Carpenter SB, Becker CE, Ediriweera HN, Mullick AE, Golenbock DT, Stuart LM. CD36 coordinates NLRP3 inflammasome activation by facilitating intracellular nucleation of soluble ligands into particulate ligands in sterile inflammation. *Nat Immunol.* 2013; 14:812–820. published online EpubAug. DOI: 10.1038/ni.2639 [PubMed: 23812099]
 28. Bretscher P, Egger J, Shamshiev A, Trotschmuller M, Kofeler H, Carreira EM, Kopf M, Freigang S. Phospholipid oxidation generates potent anti-inflammatory lipid mediators that mimic structurally

- related pro-resolving eicosanoids by activating Nrf2. *EMBO molecular medicine*. 2015; published online EpubMar 13. doi: 10.15252/emmm.201404702
29. Hornung V, Latz E. Intracellular DNA recognition. *Nature reviews. Immunology*. 2010; 10:123–130. published online EpubFeb. DOI: 10.1038/nri2690
30. Miyake Y, Yamasaki S. Sensing necrotic cells. *Adv Exp Med Biol*. 2012; 738:144–152. DOI: 10.1007/978-1-4614-1680-7_9 [PubMed: 22399378]
31. Lande R, Gregorio J, Facchinetti V, Chatterjee B, Wang YH, Homey B, Cao W, Wang YH, Su B, Nestle FO, Zal T, et al. Plasmacytoid dendritic cells sense self-DNA coupled with antimicrobial peptide. *Nature*. 2007; 449:564–569. published online EpubOct 4. DOI: 10.1038/nature06116 [PubMed: 17873860]
32. Koulis C, Chen YC, Hausding C, Ahrens I, Kyaw TS, Tay C, Allen T, Jandeleit-Dahm K, Sweet MJ, Akira S, Bobik A, et al. Protective role for Toll-like receptor-9 in the development of atherosclerosis in apolipoprotein E-deficient mice. *Arteriosclerosis, thrombosis, and vascular biology*. 2014; 34:516–525. published online EpubMar. DOI: 10.1161/ATVBAHA.113.302407
33. Horibata S, Coonrod SA, Cherrington BD. Role for peptidylarginine deiminase enzymes in disease and female reproduction. *The Journal of reproduction and development*. 2012; 58:274–282. [PubMed: 22790870]
34. Goossens P, Gijbels MJ, Zerneck A, Eijgelaar W, Vergouwe MN, van der Made I, Vanderlocht J, Beckers L, Buurman WA, Daemen MJ, Kalinke U, et al. Myeloid type I interferon signaling promotes atherosclerosis by stimulating macrophage recruitment to lesions. *Cell Metab*. 2010; 12:142–153. published online EpubAug 4. DOI: 10.1016/j.cmet.2010.06.008 [PubMed: 20674859]
35. Rathinam VA, Vanaja SK, Waggoner L, Sokolovska A, Becker C, Stuart LM, Leong JM, Fitzgerald KA. TRIF licenses caspase-11-dependent NLRP3 inflammasome activation by gram-negative bacteria. *Cell*. 2012; 150:606–619. published online EpubAug 3. DOI: 10.1016/j.cell.2012.07.007 [PubMed: 22819539]
36. Broz P, Ruby T, Belhocine K, Bouley DM, Kayagaki N, Dixit VM, Monack DM. Caspase-11 increases susceptibility to Salmonella infection in the absence of caspase-1. *Nature*. 2012; 490:288–291. published online EpubOct 11. DOI: 10.1038/nature11419 [PubMed: 22895188]
37. Khandpur R, Carmona-Rivera C, Vivekanandan-Giri A, Gizinski A, Yalavarthi S, Knight JS, Friday S, Li S, Patel RM, Subramanian V, Thompson P, et al. NETs Are a Source of Citrullinated Autoantigens and Stimulate Inflammatory Responses in Rheumatoid Arthritis. *Sci Transl Med*. 2013; 5:178ra140. published online EpubMar 27. doi: 10.1126/scitranslmed.3005580
38. Metzler KD, Fuchs TA, Nauseef WM, Reumaux D, Roesler J, Schulze I, Wahn V, Papayannopoulos V, Zychlinsky A. Myeloperoxidase is required for neutrophil extracellular trap formation: implications for innate immunity. *Blood*. 2011; 117:953–959. DOI: 10.1182/blood-2010-06-290171 [PubMed: 20974672]
49. Aga E, et al. Inhibition of the spontaneous apoptosis of neutrophil granulocytes by the intracellular parasite *Leishmania major*. *J Immunol*. 2002; 169:898–905. [PubMed: 12097394]
50. Piedrahita JA, et al. Generation of mice carrying a mutant apolipoprotein E gene inactivated by gene targeting in embryonic stem cells. *Proceedings of the National Academy of Sciences of the United States of America*. 1992; 89:4471–4475. [PubMed: 1584779]

One Sentence Summary

Cholesterol crystals trigger NETosis to prime macrophages for cytokine production in sterile atherosclerotic inflammation.

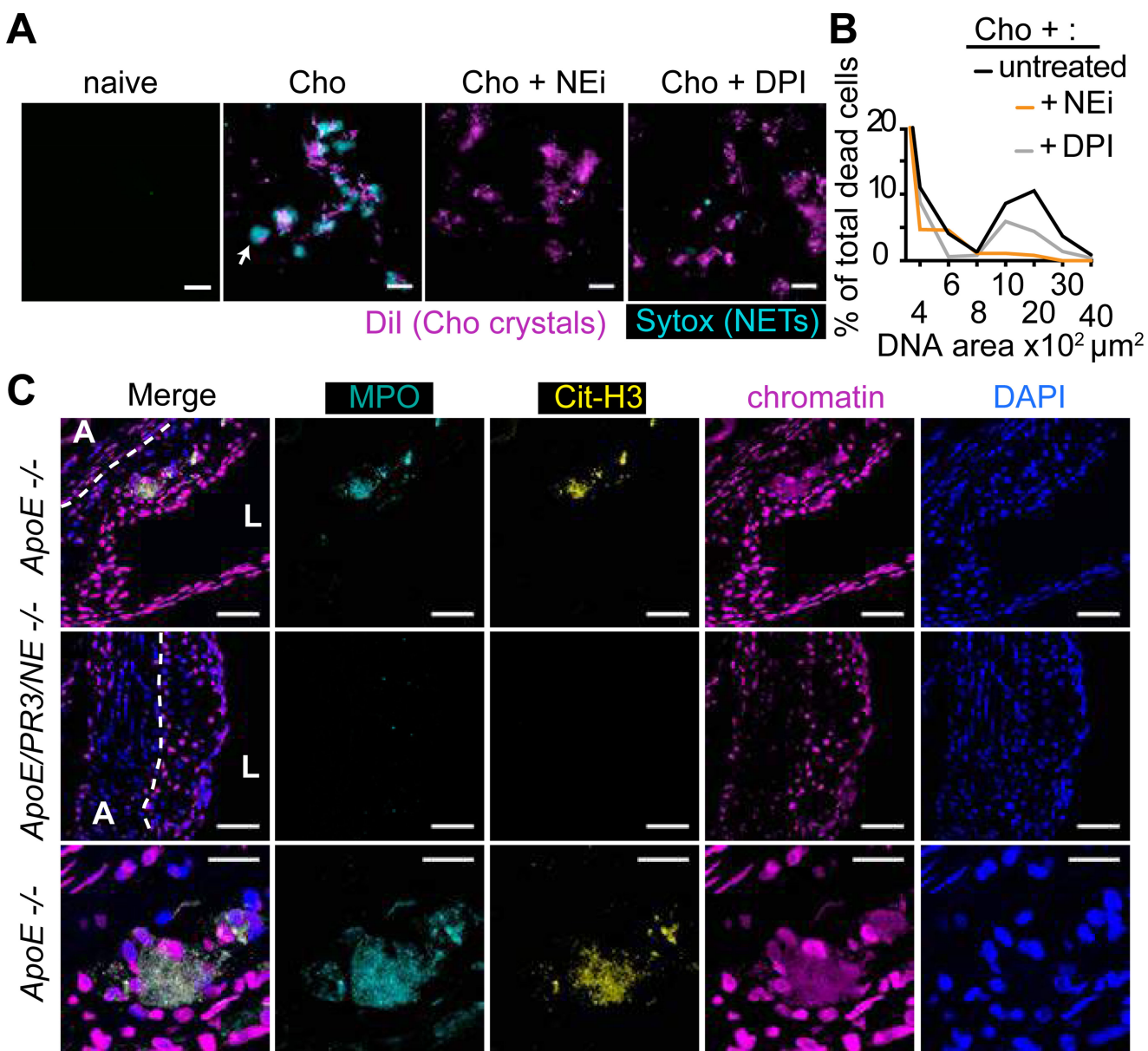


Figure 1. Cholesterol crystals trigger NETosis.

(A) Fluorescence micrograph of neutrophils incubated with cholesterol crystals and stained with the lipid dye Dil (red) and extracellular DNA (Sytox, green). Neutrophils were left untreated or treated with NE inhibitor (NEi) or the NADPH oxidase inhibitor DPI. Scale bar: 100 μm . (B) Quantitation of NETosis in (A). Data are representative of 3 independent experiments. (C) Representative confocal immunofluorescence microscopy images of aortic root sections from *ApoE*^{-/-} and *ApoE/NE/PR3*^{-/-} mice placed on HFD for 8 weeks and stained for MPO (cyan), citrullinated histone 3 (cit-H3, yellow), chromatin (magenta) and DNA (DAPI, blue). Border between the adventitia (A) and the lesion (dotted line) and lumen (L) are shown. Scale bar: 50 μm . The third row shows detail of the white boxed area

showing NETs (arrow) Scale bar: 20 μm . Representative data of 8 mice analyzed per strain from 2 independent experiments.

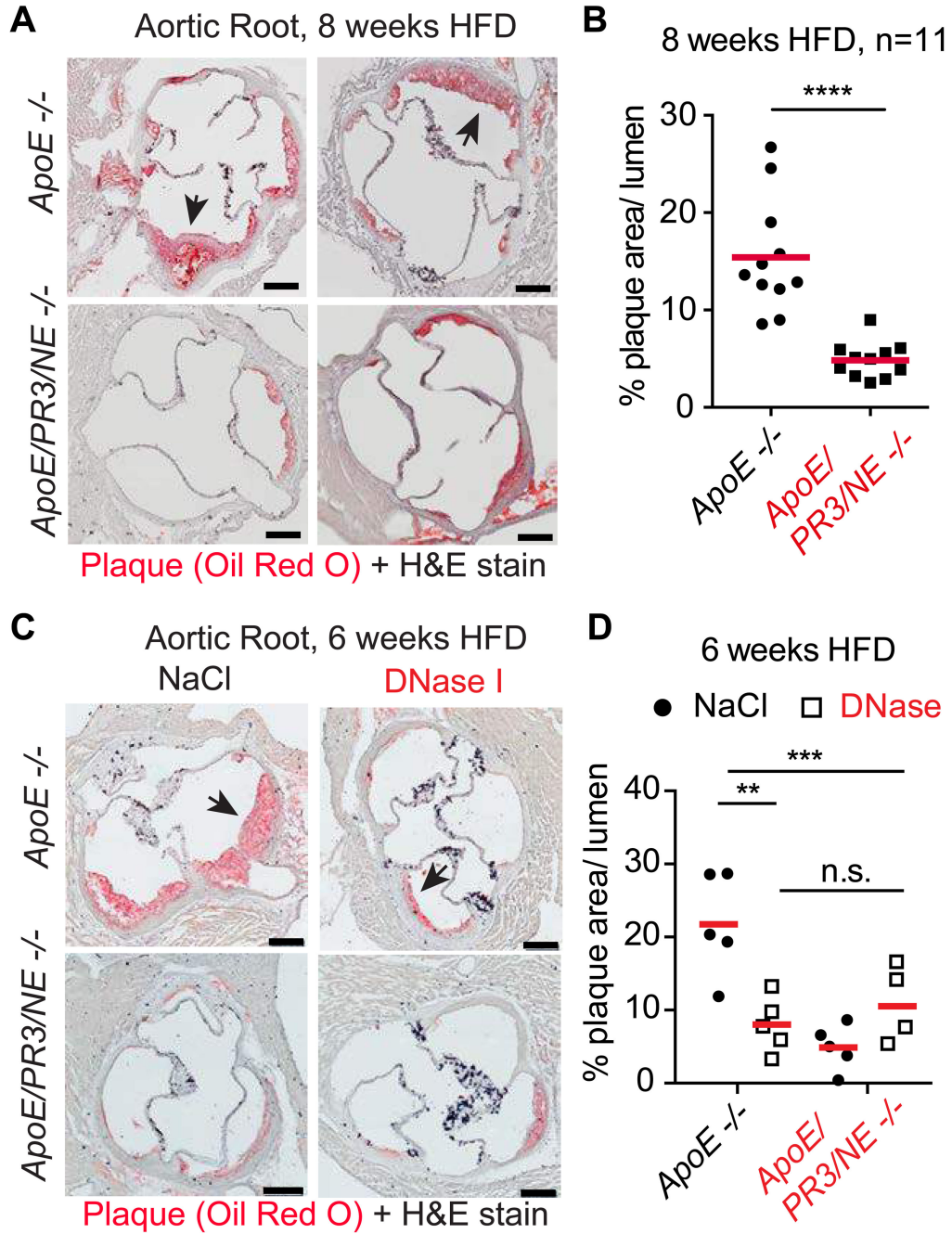


Figure 2. NETs promote atherosclerosis.

(A) Two representative microscopy images of aortic root sections from *ApoE*^{-/-} and *ApoE/NE/PR3*^{-/-} mice placed on HFD for 8 weeks and stained for lipid (Oil Red O, red) and Haematoxylin. (B) Quantitation of plaque area relative to the area of the aortic lumen from (A). Representative data of 11 mice per strain pooled from 2 independent experiments. Each point is the mean from multiple sections per animal (C) Representative microscopy images of aortic root sections from *ApoE*^{-/-} and *ApoE/NE/PR3*^{-/-} mice placed on HFD for 6 weeks and regularly injected intravenously with 120U DNase or vehicle control 0.9%

NaCl. Stained for lipid (Oil Red O, red) and Haematoxylin. **(D)** Quantitation of **(C)** as in **(B)**. Representative data of 4 or 5 mice analysed per strain and condition. A power analysis revealed 92% power for the difference of means between 0.9% NaCl- and DNase-treated *ApoE*^{-/-} mice. Statistics by Student's *t*-test for single comparison and two-way ANOVA, followed by Sidak's multiple comparison post test for multiple comparisons: * $p < 0.05$, ** $p < 0.01$, *** $p < 0.001$, **** $p < 0.0001$.

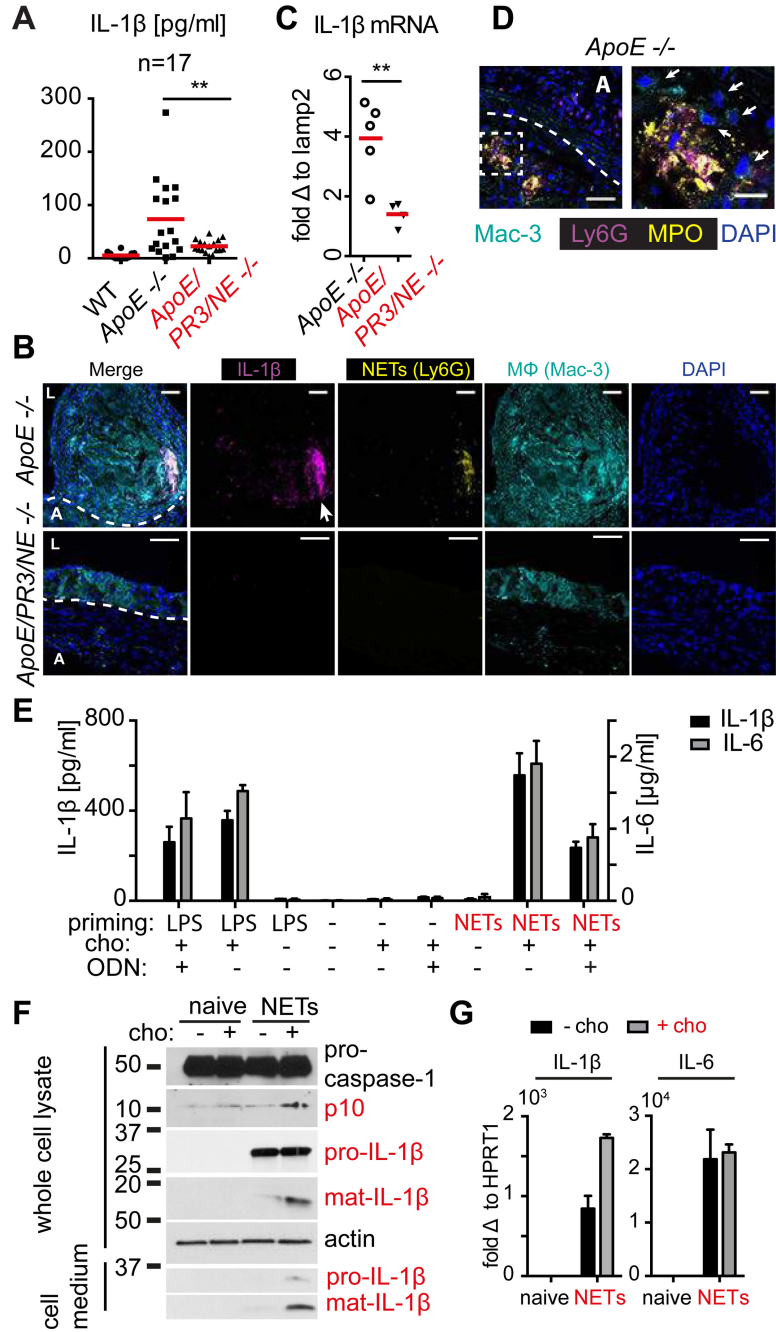


Figure 3. NETs prime macrophages for cytokine release. (A) Plasma levels of IL-1β from WT, *ApoE*^{-/-} and *ApoE/NE/PR3*^{-/-} on HFD for 8 weeks, measured by ELISA in n=17 mice per strain pooled from three independent experiments. (B) Representative confocal immunofluorescence microscopy images of aortic root sections from 8 *ApoE*^{-/-} and 5 *ApoE/NE/PR3*^{-/-} mice in 2 independent experiments placed on HFD for 8 weeks and stained with the macrophage marker Mac-3 (cyan), IL-1β (magenta), the neutrophil marker Ly6G (yellow) and DNA (DAPI, blue). Dotted line denotes the adventitia (A) / lesion boundary and (L) the lumen. Scale bars: 50 μm (C) Representative IL-1β mRNA

levels in aorta of 5 *ApoE*^{-/-} and 4 *ApoE/NE/PR3*^{-/-} mice repeated in 2 independent experiments where fed on HFD for 8 weeks measured by qPCR. mRNA levels were normalized to the monocyte/macrophage specific gene *lamp2* and expressed relative to levels measured in WT mice. A power analysis measured 89% power for the difference of means between *ApoE*^{-/-} and *ApoE/PR3/NE*^{-/-} mice. **(D)** Representative confocal immunofluorescence microscopy images of aortic root sections from 5 *ApoE*^{-/-} mice placed on HFD for 8 weeks and stained with the macrophage marker Mac-3 (cyan), MPO (magenta), citrullinated histone 3 (Cit-H3, yellow) and DNA (DAPI, blue). Scale bars: 50 μ m. Right panel is a close-up of the highlighted area of the left panel and arrows point to macrophages. Scale bars: 20 μ m. **(E)** Mature IL-1 β (black bars, left y axis) or IL-6 (grey bars, right y-axis) protein released by CD-14 blood-derived human monocytes untreated or treated with LPS or NETs alone or in the presence of cholesterol crystals. Where indicated, cells were treated with 10 μ g/ml oligonucleotide inhibitor (ODN). **(F)** Whole cell lysates or cell culture medium from naïve CD-14 blood-derived human monocytes or treated with NETs alone (black bars) or in the presence of cholesterol crystals (grey bars) analyzed by SDS-PAGE electrophoresis and immunoblotted for IL-1 β , caspase-1 and actin. **(G)** IL-1 β (left panel) or IL-6 (right panel) mRNA in naïve CD-14 blood-derived human monocytes or treated with NETs alone (black bars) or in the presence of cholesterol crystals (grey bars). **(E-G)** Representative data of 3 independent experiments with standard error across 3 technical replicates. Statistics by Student's *t*-test for single comparison and two-way ANOVA, followed by Sidak's multiple comparison post test for multiple comparisons: * $p < 0.05$, ** $p < 0.01$, *** $p < 0.001$, **** $p < 0.0001$.

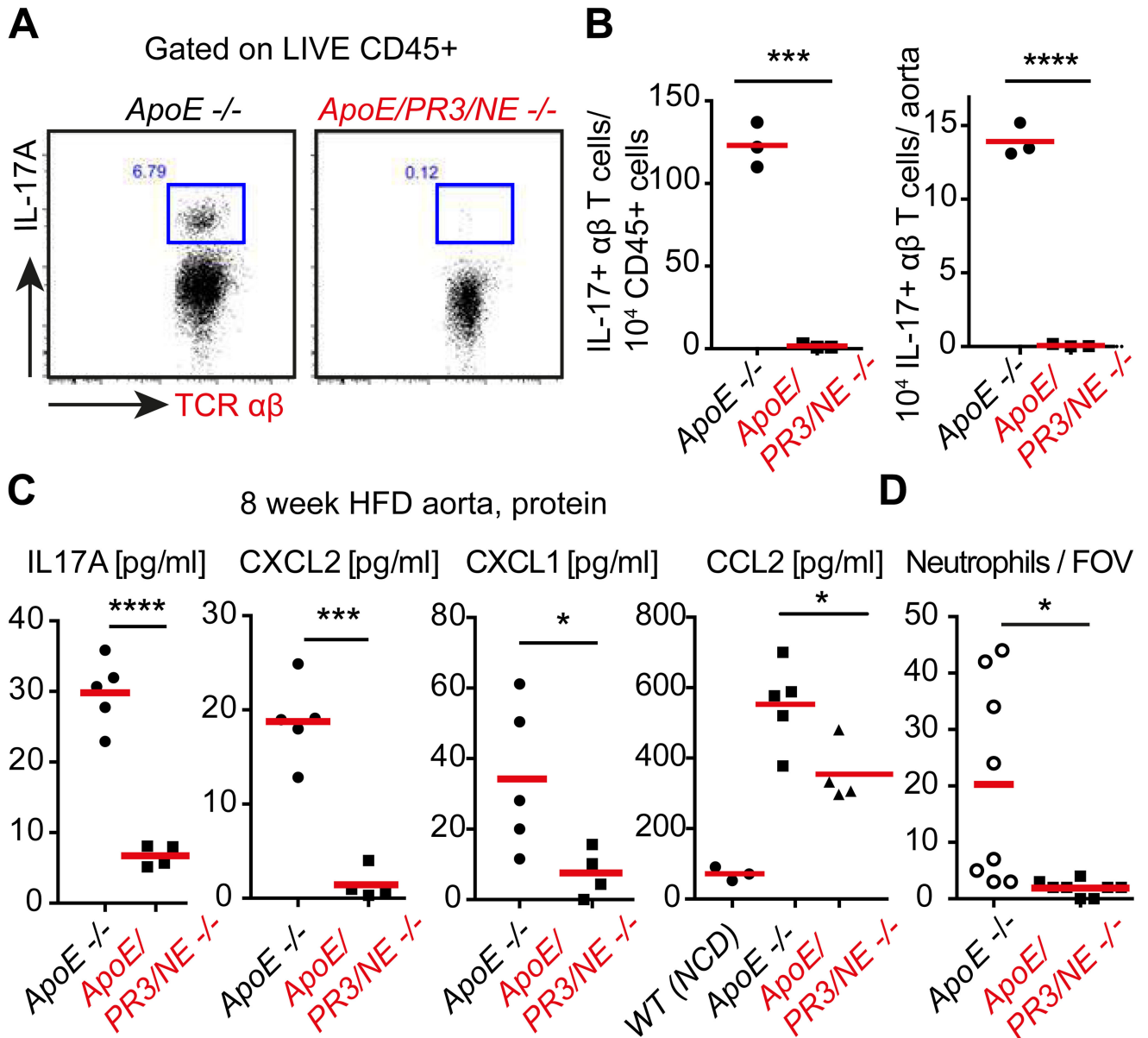


Figure 4. NETs drive IL-17 and neutrophil chemokine production in atherosclerosis.

(A) Representative FACS plot of IL-17 intracellular staining in $\alpha\beta$ and $\gamma\delta$ T cells from PMA-restimulated digested aortas of *ApoE*^{-/-} or *ApoE/PR3/NE*^{-/-} mice on HFD for 8 weeks. (B) Representative number of cells relative to CD45+ populations and whole aortas from (A) for 3 animals per group repeated in two independent experiments. (C) IL-17A, CXCL1, CXCL2 and CCL2 concentrations from whole aorta samples measured by ELISA. N=5 *ApoE*^{-/-} and n=4 *ApoE/PR/NE*^{-/-} mice. (D) Number of total intact Ly6G-stained neutrophils per aortic root section field of view (FOV) measured in immunostained micrographs. 8 mice per strain in 2 independent experiments. Statistics by two-tailed, unpaired Student's *t*-test: * *p*<0.05, ** *p*<0.01, *** *p*<0.001, **** *p*<0.0001.